an ash layer can develop an imbricate pattern, leaving gaps in lateral continuity. Such gaps might account for failure to encounter an ash bed and for difficulties in the correlation of ash beds in drill cores (*9*). Missing ash beds could result in the misidentification of tephra layers where the criteria for recognition include the position or number of ash beds in a sequence.

ROGER Y. ANDERSON
Department of Geology, University of New Mexico, Albuquerque 87131

EDWARD B. NUHFER
Department of Geosciences, University of Wisconsin, Platteville 53818

WALTER E. DEAN
U.S. Geological Survey, Denver, Colorado 80225

References and Notes

1. E. B. Welch, M. D. Tomasek, S. B. Lazoff, in *Proceedings of the conference on Mount St. Helens: Effects on water resources* (Report 41, Washington Water Research Center, Pullman, 1982), pp. 404–422.
2. E. B. Welch, M. D. Tomasek, D. E. Spyridakis, "Stability of the Mount Saint Helens' ashlayer in Moses Lake" (unpublished) (report of the Department of Civil Engineering, University of Washington, Seattle, 1983).
3. M. A. Hampton, *J. Sediment. Pet.* **42** (No. 4), 775 (1972).
4. J. D. Sims, *Tectonophysics* **29**, 141 (1975).
5. Ph. H. Kuenen, *Trans. Geol. Soc. Glasgow* **23**, 1 (1958).
6. ——, *Geol. Mijnbouw* **44e**, 22 (1965).
7. R. Y. Anderson, *Limnol. Oceanogr.* **22**, 423 (1977).
8. P. J. Mehringer, Jr., E. Blinman, K. L. Petersen, *Science* **198**, 257 (1977).
9. J. D. Sims, in *Paleolimnology of Lake Biwa and the Japanese Pleistocene*, S. Horie, Ed. (1976), vol. 4, pp. 658–702.
10. A. M. Sarna-Wojcicki *et al.*, *U.S. Geol. Surv. Prof. Pap. 1250* (1981), pp. 577–600.
11. We are indebted to G. Del Mastro, L. Habenicht, L. Smith, and S. Adams for assistance in the field and laboratory. Supported by NSF grant EAR81-13072.

27 February 1984; accepted 12 April 1984

Resonant Nuclear Fusion Processes and the Gamma Rays of SS 433

Abstract. *Gamma-ray spectral lines have recently been reported coming from the celestial object SS 433, which is known to emit high-speed jets in opposite directions. The proposed identification of the lines as coming from fusion reactions on nitrogen nuclei as part of the carbon-nitrogen-oxygen cycle operating in the jets has now received observational support. Predictions of strengths and widths of additional lines which, if seen, would provide valuable new information about conditions giving rise to the jets are presented.*

The galactic object V 1343 Aql (better known as SS 433) exhibits two sets of optical spectral lines which move back and forth across the spectrum (*1*). These lines have generally been interpreted as Doppler-shifted emissions from the two collimated jets ejected at a speed near one fourth that of light (*2*). The high-resolution γ-ray detector on the HEAO-3 satellite (*3*) detected clearly defined γ-ray spectral lines from the general direction of SS 433 at energies of 1.2 and 1.5 MeV. This in itself is remarkable: although nuclear γ-ray production does occur in stellar interiors, the original energy signatures of these spectral lines would be lost long before they reached the surface.

The γ-rays from SS 433 were initially interpreted by Lamb *et al.* (*4*) as Doppler-shifted components of a 1.37-MeV γ-ray line from inelastically excited ^{24}Mg nuclei. Their appearance was correlated (*5*) with a flare observed in radio waves and in x-rays (*6*) from SS 433. An analysis by Boyd *et al.* (*7*), referred to hereafter as BWNC, has shown the magnesium interpretation to be unlikely on the basis of the prodigious power [observed by Lamb *et al.* (*4*) to be about 10^{37} ergs per second per jet] contained in the observed narrow γ-ray lines. Alternatively, Ramaty *et al.* (*8*) suggested that the observed γ-rays might be produced by collisions of grains in the jets with the surrounding medium.

The BWNC study suggested that the γ-rays could be produced by the ^{14}N(p,γ)^{15}O nuclear fusion reaction taking place in the jets. It produces a 1.38-MeV γ-ray line from a resonance reaction process which occurs when the proton has an energy with respect to the ^{14}N nucleus of ~280 keV. Thus most of the energy observed in the γ-ray lines results from the energy released by the nuclear reactions, not from the kinetic energy of the jets. Then the power output in the γ-ray lines is

$$P_\gamma = [\mathrm{H}]\,[\mathrm{N}] < \sigma v > BVE_\gamma$$

where [H] and [N] are the number densities of H and N, respectively; $< \sigma v >$ is the thermonuclear reaction rate; B is the branching ratio, which provides the 1.38-MeV line; V is the volume of the emitting region; and E_γ is the energy of a γ-ray photon. The thermonuclear reaction rates were taken to be those of Fowler *et al.* (*9*).

However, it was noted that one assumption inherent in those rates, namely, that the relative energies of protons and ^{14}N nuclei were characterized by a Boltzmann distribution, might not apply. Indeed, most of the proton-^{14}N energy difference probably results from differential acceleration of the two species. For example, if that acceleration mechanism is electromagnetic, the acceleration will depend on the charge-to-mass ratio; this will be about twice as large for protons as for all other nuclear species (assuming nearly complete electron stripping). The buildup of large energy differences is limited by collisions of the jet protons with the other constituents. The competition between unrestricted acceleration and collisional equilibration, together with cooling via coupling to the electrons, could produce a fairly narrow proton-^{14}N energy distribution peaked at a fairly large value. The result of this non-Boltzmann distribution could be a large enhancement in the reaction rate, hence in P_γ, for given jet densities.

The essential feature for production of a line by this mechanism is that a resonant process exist. Otherwise the γ-rays produced will be distributed over a wide range in energy, thus obscuring any well-defined γ-ray peaks. This point is illustrated in Fig. 1, where the ^{14}N(p,γ) reaction is used as an example. The protons achieve a higher speed (solid curve) at any point of the acceleration region than the ^{14}N nuclei (dashed curve). As the accelerating force diminishes with distance, collisions eventually reduce the differences in flow velocity to zero. If γ-rays can be produced over a large fraction of that region, they will have a large range of velocities, hence Doppler-shifted energies. However, if the reaction cross section between protons and ^{14}N nuclei resonates at some energy, then γ-rays will primarily be emitted at the point at which the relative velocity (dotted curve) equals the velocity corresponding to the resonant energy (horizontal line). Conceivably two peaks could thus result, although differences in density and location of the two emitting regions should reduce the output from one of them greatly with respect to the other.

We have considered possible reactions on the carbon-nitrogen-oxygen cycle nuclei and have listed the strongest lines, at energies E_γ, together with their resonant proton-nucleus energies E_{res}, in Table 1. Also listed are estimates of the intensity of each line relative to that of the 1.38-MeV line (column labeled I^{rel}). Factors necessary for determining the relative intensities are the branching ratio B, the thermonuclear reaction rate $< \sigma v >$ multiplied by Avogadro number N_A, and the number fraction X/A of the nucleus which initiated the reaction. The latter numbers were those obtained by Boyd *et al.* (*7*) for nucleosynthesis times long enough to permit equilibrium to be achieved, about 3×10^4 seconds for the conditions assumed for figure 1 of (*7*). Also included in Table 1 are the widths of the resonances Δ, which, when combined with the detector resolution, give the observed line widths.

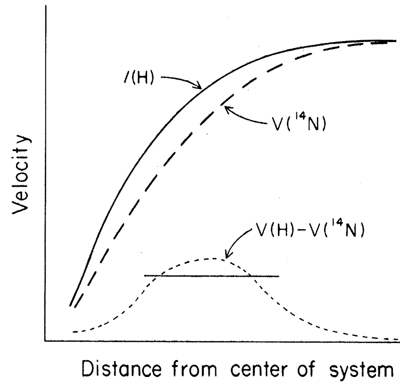

Fig. 1. Schematic description of the velocities of protons and nitrogen nuclei versus the distance from the center of the system for the case in which the acceleration mechanism depends on the charge-to-mass ratio. (The absolute scales are not known at present.) The solid curve gives the proton velocity, the dashed curve the ^{14}N velocity, and the dotted curve their relative velocity. Regions of high γ-ray yield via the $^{14}N(p,\gamma)^{15}O$ reaction can occur at the intercepts of the velocity corresponding to the resonance (horizontal line) with the relative velocity curve.

All the resonances indicated in Table 1 do not occur at the same relative proton-nucleus energy. Thus they might reach their γ-ray production peaks in different regions of the jets, where different proton-nucleus energies, and probably densities, would prevail. Indeed the maximum relative energy might not even be large enough to excite all the resonances. An additional uncertainty results from the fact that the distributions may, as noted earlier, differ appreciably from the Boltzmann form. Anisotropies in the γ-ray angular distributions might also produce some departure from the predicted strengths. Nonetheless, we have obtained a rough estimate of the relative line strengths, assuming a single temperature, $T = 1 \times 10^9$ K. In spite of the uncertainties discussed above, we feel the present predictions to be at least qualitatively correct: the reactions that produce strong lines in carbon-nitrogen-oxygen burning would be expected to do so also in the jets of SS 433 as long as the resonance energies are less than the maximum proton-nucleus energy differences. The predicted strengths provide a test of the BWNC model: the four lines produced in the ^{14}N (p,γ) reaction must occur with the intensity given in Table 1 because they are produced by the same resonance. Indeed, the prediction of the BWNC model that each 1.38-MeV γ-ray should be accompanied by a 6.18-MeV secondary has recently received support from Lamb *et al.* (*5*) in their probable detection of the blue-shifted member of the secondary. However, significant departures from the predicted relative strengths could occur for other lines: the amount of deviation from the predicted strengths could be useful in learning about the variation in proton-nucleus energy differences in different regions of the jets.

The actual energy at which a line is observed is closely tied to the mechanism by which the associated γ-rays are produced. For example, a variety of spectral lines could result from transitions from the ^{14}N(2.31-MeV) state to the ^{14}N(ground) state. The BWNC model predicts a strong component of ^{14}N in the jets; the collision of this nitrogen with the hydrogen of the gas in the interstellar medium surrounding SS 433 could produce γ-rays from de-excitation of the collisionally excited ^{14}N. Sharp peaks exist in the cross section (*10*) for $^{14}N(p,p')^{14}N$(2.31 MeV) at $E_p = 3.9$ and 4.9 MeV. Thus 2.31-MeV γ-rays might be expected with $v/c \sim 0.1$, where c is the speed of light. However, the analysis of Boyd *et al.* (*7*) of a similar process for production of the magnesium line suggests that the power in such lines would be far below observational limits.

The surrounding gas is also thought to be unusually rich in nitrogen (*11*). Thus collisions of the hydrogen in the jets with the stationary nitrogen could produce a virtually unshifted, but fairly broad, 2.31-MeV γ-ray line from these 3.9- and 4.9-MeV peaks; its tentative identification has been reported by Lamb (*12*). Both mechanisms discussed above involve collisions with the gas of the surrounding medium and so involve properties of that gas that do not occur in considerations of the power output for the fusion reaction processes. Thus the relative intensities of the lines they produce cannot be determined with respect to the lines of the carbon-nitrogen-oxygen cycle.

Observation of highly Doppler-shifted components of the 2.31-MeV line could signal the occurrence in the jets of $^{13}N(p,\gamma)^{14}O$, a reaction central to the rp, or rapid proton burning, process (*13*). That reaction resonates at an energy of 550 keV and is followed by positron decay to the ^{14}N(2.31 MeV) state. It would also produce (*14*) a 5.17-MeV γ-ray from ^{14}O. The ^{13}N(p,γ) process can occur only if the fusion reactions occur so rapidly that the ^{13}N produced in the ^{12}C(p,γ) reaction does not have time to beta-decay before conversion to ^{14}O; this could occur at high jet densities (*7*). Since the width of the shifted 2.31-MeV lines would depend on the change in velocity of the ^{14}O nuclei over the 70.6-second half-life of ^{14}O, they could be broad and possibly skewed if the acceleration is sufficiently rapid. Thus, if they are seen, their detailed shape might pro-

Table 1. Predicted strong γ-ray lines in the carbon-nitrogen-oxygen cycle. Only lines with predicted strengths greater than 10 percent of that for the 1.38-MeV line resulting from ^{14}N(p,γ) were included.

Reaction*	E_{res} (MeV)	Transition (MeV)	B (%)	E_γ (MeV)	$N_A < \sigma v >$ (cm^3 mol^{-1} sec^{-1})	X/A	Γ_γ^{rel}	Δ (keV)
^{14}N(p,γ)	0.28	$7.56 \rightarrow 6.18$	58	1.38	112	3.6×10^{-4}	1.00	1.6
		$7.56 \rightarrow 6.79$	23	0.77			0.40	1.6
		$7.56 \rightarrow 5.18$	16	2.38			0.28	1.6
		$6.18 \rightarrow 0.0$	58	6.18			1.00	
^{12}C(p,γ)	0.46	$2.37 \rightarrow 0.0$	100	2.37	868	4.3×10^{-5}	1.60	50
^{13}C(p,γ)	0.55	$8.06 \rightarrow 0.0$	80	8.06	3720	1.0×10^{-5}	1.27	30
		$8.06 \rightarrow 3.95$	13	4.11			0.21	30
		$3.95 \rightarrow 2.31$	12	1.64			0.20	
		$2.31 \rightarrow 0.0$	12	2.31			0.20	
^{16}O(p,γ)	No	$0.50 \rightarrow 0.0$	80	0.50	4	5.4×10^{-4}	0.07	
^{13}N(p,γ)	0.54	$5.17 \rightarrow 0.0$	100	5.17	(300)	See text	<1.60	40
$^{14}O \rightarrow {}^{14}N$	No	$2.31 \rightarrow 0.0$	100	2.31	(300)	See text	<1.60	See text
^{14}N(p,p')	No	$2.31 \rightarrow 0.0$	100	2.31		See text		

*For the ^{16}O(p,γ) reaction, the information for cumulative branching ratios and transitions came from (*15*). For all other reactions, that information came from (*16*).

vide a way of determining the accelerating field experienced by the jets.

Observation of the γ-rays from SS 433 has apparently allowed us to observe the occurrence of some of the fusion processes normally occurring only in the stellar interior. These same data might also provide extremely detailed information about some of the properties of that stellar system. Whether the existing data are good enough for such inferences or not, this one experiment certainly gives strong impetus for further high-spectral-resolution γ-ray astronomy experiments, both to refine our understanding of SS 433 and to search for other stellar objects from which similarly detailed information could be obtained. Systems from which γ-rays of well-defined energies might be emitted would certainly include objects known to have both jets and x-ray emission, such as the quasar 3C273, the peculiar galaxy M87, and the galactic x-ray source G109.1-1.0.

R. N. Boyd

Department of Physics, Ohio State University, Columbus 43210

G. H. Newsom
G. W. Collins II

Department of Astronomy, Ohio State University

M. Wiescher

Institut für Kernchemie, Johannes Gutenberg-Universität, Mainz, West Germany

References and Notes

1. A. Mammano, F. Ciatti, A. Vittone, *Astron. Astrophys.* **85**, 14 (1980); B. Margon, *Ann. N.Y. Acad. Sci.* **336**, 550 (1978).
2. M. Milgrom, *Astron. Astrophys.* **76**, L3 (1979); G. O. Abell and B. Margon, *Nature (London)* **279**, 701 (1979).
3. W. A. Mahoney, J. C. Ling, A. S. Jacobson, *Nucl. Instrum. Methods* **185**, 449 (1981); ——, R. M. Tapphorn, *ibid.* **178**, 363 (1980).
4. R. C. Lamb, J. C. Ling, W. A. Mahoney, G. R. Riegler, W. A. Wheaton, A. S. Jacobson, *Nature (London)* **305**, 37 (1983).
5. R. C. Lamb [*Bull. Am. Astron. Soc.* **15**, 991 (1983)] reports on recent results of R. C. Lamb, J. C. Ling, W. A. Mahoney, G. R. Riegler, W. A. Wheaton, and A. S. Jacobson.
6. E. R. Seaquist, W. S. Gilmore, K. J. Johnston, J. E. Grindlay, *Astrophys. J.* **260**, 220 (1982).
7. R. N. Boyd, M. Wiescher, G. H. Newsom, G. W. Collins II, *ibid.* **276**, L9 (1984).
8. R. Ramaty *et al.*, *ibid.*, in press.
9. W. A. Fowler, G. R. Caughlan, B. A. Zimmerman, *Annu. Rev. Astron. Astrophys.* **13**, 69 (1975).
10. M. L. West, C. M. Jones, J. K. Bair, H. K. Willard, *Phys. Rev.* **179**, 1047 (1969).
11. R. P. Kirshner and R. A. Chevalier, *Astrophys. J.* **242**, L77 (1980), and references therein.
12. R. C. Lamb, personal communication.
13. R. K. Wallace and S. E. Woosley, *Astrophys. J. Suppl. Ser.* **45**, 389 (1981).
14. M. J. Harris, W. A. Fowler, G. R. Caughlan, B. A. Zimmerman, preprint, 1983.
15. F. Ajzenberg-Selove, *Nucl. Phys. A* **375**, 1–168 (1982).
16. ——, *ibid.* **360**, 1–186 (1981).
17. We thank R. C. Lamb and A. S. Jacobson for helpful discussions on details of the x-ray data. This work was supported in part by NSF grant PHY 8203699.

19 March 1984; accepted 16 May 1984

A New Ribosome Structure

Abstract. *Ribosomes derived from the sulfur-dependent archaebacteria are structurally distinct from those types found in ribosomes from eubacteria, eukaryotes, and other archaebacteria. All four ribosome types share a common structural core, but each type also has additional independent structural features. In the smaller subunit derived from sulfur-dependent archaebacteria ("eocytes"), lobes, similar to those found at the base of the eukaryotic small subunits, and an archaebacterial bill, similar to those found on the smaller subunit of archaebacteria and eukaryotes, are present. On the larger subunit from sulfur-dependent archaebacteria, an eocytic lobe, eocytic gap, and eocytic bulge are present. These features, with the exception of the eocytic gap, are found in a slightly modified form on eukaryotic large subunits. These novel ribosomal properties are in general consistent with other molecular biological properties peculiar to these organisms.*

In recent years, our understanding of the diversity of the fundamental molecular processes found in living organisms has expanded. Numerous data collected on fundamental cellular properties of diverse organisms seem to fall into a few patterns (*1*). In particular, ribosomes from organisms within the eubacterial, archaebacterial, and eukaryotic lineages each have different three-dimensional structures (*2*). We now report an unusual fourth type of ribosomal structure found in the sulfur-dependent archaebacteria ("eocytes") (*3*) that thrive in thermal springs at temperatures above 90°C (*4*, *5*).

Small ribosomal-subunits from five representative sulfur-dependent archaebacteria (eocytes) (Fig. 1A) were compared to ribosomal subunits from eubacteria, other archaebacteria, and eukaryotes (Fig. 1B). The four types are interpreted in diagrams at the bottom of Fig. 1. The "asymmetric projection" of the small subunit is shown to facilitate comparisons. This is the same projection that has been used to analyze the three-dimensional structures of archaebacterial, eukaryotic, and eubacterial small subunits (2).

Large subunits from five representative sulfur-dependent archaebacteria (Fig. 1C) were compared to ribosomal subunits from eubacteria, other archaebacteria, and eukaryotes (Fig. 1D). The large subunits are shown in a projection that is useful for comparative purposes, the "quasisymmetric" projection (*6*). Identification of this projection of the eocytic large subunits was determined by reference to the eubacterial structure. Beneath both galleries (Fig. 1, E and F, respectively) are composite diagrams that illustrate the features of all four types of small and large subunits.

The small subunits of sulfur-dependent archaebacteria contain a feature not found in ribosomes of other bacteria. Lobes are present at the base of their small subunits so that their structure is intermediate between that of the archaebacterial and the eukaryotic small subunits. The lack of "eukaryotic lobes" in small subunits of eubacteria and other archaebacteria has been described (2). These sulfur-dependent bacterial ribosomes are the only bacterial ribosomes known to have these "eukaryotic" structures. Like the ribosomes of archaebacteria and eukaryotes, the small subunits of sulfur-dependent archaebacteria have the archaebacterial bill (*2*).

Large subunits from sulfur-dependent archaebacteria (Fig. 1C) can be recognized by an indentation, the "eocytic gap." This feature gives these ribosomes their characteristic shape by separating a region of density at the bottom of the subunit, the "eocytic lobe," from a second region on the side of the subunit, the "eocytic bulge." For example, they can be compared with the large subunit from the archaebacterium *Halobacterium cutirubrum* (central panel, Fig. 1D). In both the other archaebacteria and in eubacteria the lobe and bulge are absent, or nearly so. In the eukaryotic large subunit, both the lobe and the bulge are present, and the gap between them is filled. The "eocytic lobe and bulge" are present in the large ribosomal subunits of both the sulfur-dependent archaebacteria and eukaryotes (Fig. 1D), but the gap occurs only in ribosomes of the sulfur-dependent archaebacteria.

In many molecular properties, the sulfur-dependent archaebacteria resemble eukaryotes. Their DNA-dependent RNA polymerases are composed of protein subunits with molecular weights and immunological properties that resemble those of eukaryotic polymerase A(I) more closely than the patterns found in the halobacteria, methanogens, and eubacteria (*7*). Introns similar to those found in eukaryotic transfer RNA (tRNA) genes, have been found in tRNA genes in the sulfur-dependent bacteria *Sulfolobus* (*8*), whereas none has yet been found in other bacteria. The sec-